



Contents lists available at ScienceDirect

## Chemical Engineering Journal

journal homepage: [www.elsevier.com/locate/cej](http://www.elsevier.com/locate/cej)Chemical  
Engineering  
Journal

## Treatment of Diphenhydramine with different AOPs including photo-Fenton at circumneutral pH

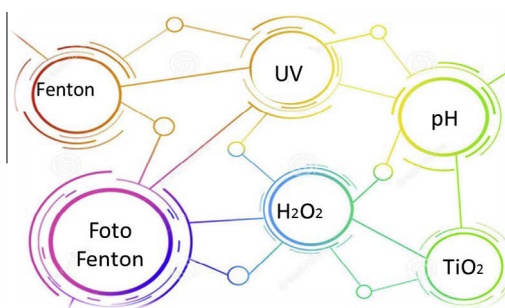
Nuria López, Sandra Plaza, Arsalan Afkhami, Pilar Marco, Jaime Giménez, Santiago Esplugas\*

Department of Chemical Engineering, Faculty of Chemistry, Universitat de Barcelona, C/Martí i Franqués 1, 08028 Barcelona, Spain

## HIGHLIGHTS

- Diphenhydramine degradation by different AOPs is compared.
- Power and wavelengths of lamps are important in the contaminant degradation.
- Fenton and photo-Fenton can work at initial circumneutral pH.
- Black blue lamps gave the best results in diphenhydramine abatement.
- Acidification of the solution is avoided by the addition of Resorcinol.

## GRAPHICAL ABSTRACT



## ARTICLE INFO

Article history:  
Available online xxx

Keywords:  
Diphenhydramine hydrochloride  
Advanced oxidation process  
Circumneutral pH  
UV-A  
UV-C  
Solar radiation

## ABSTRACT

The degradation of diphenhydramine hydrochloride (DPH), via UV-vis/H<sub>2</sub>O<sub>2</sub>, Fenton, photo-Fenton and photocatalysis processes, was studied under different radiation sources. In addition, the Fenton and photo-Fenton processes at acid pH and circumneutral pH have been compared. The importance of the source of irradiation, UV-C ( $\lambda = 254$  nm), black blue lamps (BLB,  $\lambda = 365$  nm) and simulated solar radiation (SB, SolarBox), was investigated at lab-scale. Moreover, compound parabolic collectors (CPC), at pilot plant scale with sunlight, have been also applied in photocatalytic treatments. Photo-Fenton process employing black blue lamps gave the best DPH abatement (100% of DPH conversion at 10 min for acid pH and 20 min for circumneutral pH), using the highest Fe<sup>2+</sup> (5 mg/L) and H<sub>2</sub>O<sub>2</sub> (150 mg/L) concentrations at 50 mg/L of initial DPH concentration. Using Fenton, 100% of DPH conversion was reached at 30 min for both pHs tested. In the case of UV-C/H<sub>2</sub>O<sub>2</sub>, 100% of DPH elimination was achieved in 20 min using 150 mg/L of H<sub>2</sub>O<sub>2</sub>. In the photocatalytic process, using 0.4 g TiO<sub>2</sub>/L, after 60 min of irradiation, only 35.7% and 8.7% of DPH conversion have been obtained in SB and CPC, respectively. The DPH degradation in the photocatalytic process was greatly enhanced adding H<sub>2</sub>O<sub>2</sub>. In all the cases, increasing the H<sub>2</sub>O<sub>2</sub> dose enhances the reaction rate due to higher OH<sup>•</sup> production. However, not significant mineralization was obtained. The highest DPH mineralization was 36.8% and 38.5% of TOC reduction with photo-Fenton in BLB lamps using 150 mg/L of H<sub>2</sub>O<sub>2</sub> and 2.5 mg/L of Fe<sup>2+</sup>, for acid pH and circumneutral pH, respectively. The major reaction intermediates in these processes were identified by ionization/mass spectrometry and a DPH photo-degradation structure was proposed.

© 2016 Elsevier B.V. All rights reserved.

## 1. Introduction

Water is fundamental to survival on earth. In the last years, water scarcity and water quality have become a worldwide concern. Every day large amounts of water are contaminated by differ-

\* Corresponding author.  
E-mail address: [santi.esplugas@ub.edu](mailto:santi.esplugas@ub.edu) (S. Esplugas).

ent pollutants coming from domestic or industrial uses. Although pollution of rivers by heavy metals and other compounds, strictly regulated by Dangerous Substances Directive (2006/11/EEC), is generally decreasing, organic substances with harmful properties such as pharmaceuticals and personal care products are increasingly detected in the environment [1]. Spain is ranked as one of the world's largest consumer of pharmaceuticals [2]. According to Miranda [3] these compounds are also recalcitrant and present properties of bioaccumulation in the environment. They are also resistant to conventional wastewater treatments and are found in effluents at concentrations ranging from 0.1–20.0 µg/L [3–5].

Among those pollutants, there is a special group of pharmaceuticals, antihistaminic drugs, found in water. Diphenhydramine hydrochloride is the classic H1 receptor antagonist that has been used in pregnancy for the treatment of allergies, nausea and vomiting as well as an analgesic adjuvant in cancer pain. DPH has relatively low molecular weight and high lipid solubility, allowing easy blood–brain barrier and placental passage [6]. Unfortunately, information on the environmental fate and toxicity to aquatic species is scarce for most pharmaceuticals [7]. The growing demand of society for the decontamination of water from various sources, materialized in regulations increasingly strict, has caused, in recent years, increasing research on methods to eliminate pharmaceuticals from wastewater, and this is the case of advanced oxidation processes (AOPs).

Advanced oxidation processes (AOPs) are environmental friendly methods based on in situ production of hydroxyl radical ( $\cdot\text{OH}$ ) as main oxidant. Hydroxyl radical is able to react non-selectively with most organic compounds [8].

The focus of this work is to evaluate the efficiency of UV-vis/ $\text{H}_2\text{O}_2$ , Fenton, photo-Fenton and photocatalysis in the degradation of Diphenhydramine under different radiation sources. Moreover, it has been studied the DPH conversion by Fenton and photo-Fenton at initial circumneutral pH. The acidification of the solution is avoided by the addition of resorcinol (RES, di-hydroxy benzene isomer) [9–11], which in addition is used to simulate organic matrix in water. RES addition also generates ferric-carboxylates complexes and avoids the precipitation of  $\text{Fe}^{3+}$  hydroxy complexes at neutral pH. The efficiency of this process was also compared with the classical Fenton and photo-Fenton process at acid pH.

## 2. Chemicals and experimental set-ups

### 2.1. Chemicals and reagents

The solution of 50 mg/L of Diphenhydramine hydrochloride ( $\text{C}_{17}\text{H}_{21}\text{NO} \cdot \text{HCl}$ , HPLC grade, purity  $\geq 98\%$  from Sigma-Aldrich) was prepared using deionized water. This high concentration (50 ppm) was selected to assure accurate measurements of concentrations and to follow TOC levels. Moreover this quite high concentration value was chosen to represent the concentrations in wastewaters coming from pharmaceutical companies (10–100 mg/L) [12,13]. Acetonitrile (analytical reagent grade from Fischer Chemical) and orthophosphoric acid (85% from Panreac Quimica) were used for HPLC analysis.  $\text{H}_2\text{O}_2$  (30% w/w, from Merck),  $\text{FeSO}_4 \cdot 7\text{H}_2\text{O}$  (PA from Panreac),  $\text{NaHSO}_3$  and MeOH (PAI from Panreac) reagents were used without further purification. Heterogeneous photocatalysis was performed using  $\text{TiO}_2$  P-25 (Evonik, Germany). Sulphuric acid ( $\text{H}_2\text{SO}_4$ , 96% purity from Panreac) was used for initial pH adjustment. Resorcinol (RES, CAS number 108-46-3) was purchased from Sigma-Aldrich.

### 2.2. Techniques and analytical instruments

DPH concentration was monitored by HPLC from Waters using a SEA18 Teknokroma column (250 × 4.6 mm i.d.; 5 µm particle size)

and a Waters 996 photodiode array detector. The mobile phase was composed by water (pH 3) and acetonitrile (70:30), injected with a flow-rate of 0.85 mL/min. DPH concentration was followed at UV maximum absorbance (220 nm). TOC was analyzed with a Shimadzu TOC-V CNS analyzer. Reproducible TOC values, with an accuracy of  $\pm 1\%$ , were obtained by injecting 50 µL samples into the analyzer.  $\text{H}_2\text{O}_2$  consumption was followed using the metavanadate spectrophotometric method at 450 nm [14].  $\text{H}_2\text{O}_2$  contained in samples was quenched with sodium hydrogen sulfite, or the same volume of methanol, to avoid further reactions depending on the analysis to be done. All samples were filtered with a polyethersulfone membrane filter (0.45 µm, Chemlab) to remove the catalyst before analytical procedures except for iron measures. The iron (II) content was determined by o-phenontraleine standardized procedure (ISO 6332).

For the intermediates identification, samples were analyzed by the electrospray ionization/mass spectrometry using an electrospray (ion spray) ESI-MS, and a LC/MSD-TOF (Agilent Technologies) mass spectrometer.

### 2.3. Experimental devices

#### 2.3.1. Artificial irradiation: UV-C reactor

The experiments with UVC lamps were performed in a thermostated Pyrex-jacketed 2 L vessel (inner diameter 11 cm, height 23 cm), equipped with three low pressure mercury lamps (Phillips TUV 8 W, G8T5) located at the center of reactor. Lamps emit monochromatic 254 nm radiation. The radiation inside the photoreactor was assessed by uranyl oxalate actinometry [15] and the obtained value was 8.01 J/s at 254 nm. A solution of DPH (50 mg/L) was introduced in the reactor and  $\text{Fe}^{2+}$  (2.5 or 5 mg/L),  $\text{H}_2\text{O}_2$  (15, 75 or 150 mg/L), RES (50 mg/L) and  $\text{TiO}_2$  (0.4 g/L) were added, depending on the AOPs studied, and immediately the lamps were switched on. Magnetic stirring was used to ensure sufficient mixing. The temperature of the solution was maintained constant at 25 °C by the jacket connected to an ultra-thermostat bath.

#### 2.3.2. Artificial irradiation: Black Blue Lamps (BLB) reactor

BLB reactor consists on a 2 L Pyrex-jacketed thermostatic vessel (inner diameter 11 cm, height 23 cm), equipped with three 8 W BLB lamps (Philips TL 8 W-08 FAM) located at the center of reactor. The lamps emit radiation between 350 and 400 nm, with a maximum at 365 nm. The radiation entering to the photoreactor was 1.97 J/s, measured by o-nitrobenzaldehyde actinometry [16]. This batch tank was fed with DPH solution (50 mg/L). Next  $\text{Fe}^{2+}$  (2.5 or 5 mg/L),  $\text{H}_2\text{O}_2$  (15, 75 or 150 mg/L), RES (50 mg/L) and  $\text{TiO}_2$  (0.4 g/L) were added depending on the advanced oxidation process. The solution was maintained at constant temperature of 25 °C; the jacket temperature of the stirred tank was controlled with an ultra-thermostat bath.

#### 2.3.3. Artificial solar irradiation: Solarbox (SB)

A Solarbox (CO.FO.ME.GRA 220V 50 Hz) with a Xenon lamp (Phillips 1 kW), located at the top of the device was used. The irradiation entering the photoreactor was 3.59 J/s measured also by o-nitrobenzaldehyde actinometry [16]. The tubular photoreactor (24 cm length, 2.11 cm diameter, Duran glass material) was placed at the bottom of the Solarbox on the axis of a parabolic mirror made of reflective aluminum. A filter cutting off wavelengths under 280 nm was placed between the lamp and the reactor. The DPH solution (50 mg/L) was prepared in a batch jacketed feeding tank (total volume 1L). Next  $\text{Fe}^{2+}$  (2.5 or 5 mg/L),  $\text{H}_2\text{O}_2$  (15, 75 or 150 mg/L), RES (50 mg/L) and  $\text{TiO}_2$  (0.05, 0.1, 0.4 g/L) were added depending on the advanced oxidation process. The solution to be treated was pumped to solarbox by peristaltic pump (Ecoline VC-280 II, Ismatec) from a stirred double jacket reservoir batch tank

(total volume 1L) with a flow-rate of 0.71 L/min. The reservoir was connected to an ultra-thermostatic bath (HaaKe K10) to assure constant temperature during the processes and all connections employed were made of Teflon to avoid losses by adsorption. A preliminary sample was collected before irradiation to represent initial concentration at 0 min, and no conversion was observed.

### 2.3.4. Solar irradiation: CPC reactor

Photocatalytic experiments were also carried out in a solar pilot plant based on compound parabolic collectors (CPC), at the University of Barcelona (latitude 41.4 N, longitude 2.1 W). The CPC consists in a module, 41° inclined, with a mirror made of polished aluminum (aluminum was chosen because it is highly reflective in the UV range: 92.3% at 280 nm to 92.5% at 385 nm), with 6 parallel tubular quartz reactors. The total mirrors area for solar irradiation capture-reflection was 0.228 m<sup>2</sup>. Experiments were done between 13:00 and 18:00 h in summer, and temperature was 30 ± 5 °C. Solar irradiation was measured by a spectroradiometer Bentham DMC300. The exposure time was enough to reach the total hydrogen peroxide consumption. The aqueous suspension of DPH was pumped with a peristaltic pump with a flow-rate 2.6 L/min, from the stirred reservoir tank (10 L) to irradiated quartz tubes and continuously recirculated. The solution was constantly mixed by RW 16 basic agitator IKA. The stirred reservoir tank (10 L) was fed with DPH solution (50 mg/L) and 0.4 g/L of TiO<sub>2</sub>, with or without H<sub>2</sub>O<sub>2</sub> (150 mg/L). A preliminary sample was collected before irradiation to represent initial concentration at 0 min, and no conversion was observed.

Table 1 shows the most important technical parameters of CPC reactor.

## 3. Results and discussions

### 3.1. Preliminary experiments: DPH adsorption and photolysis

Preliminary experiments were carried out to study the adsorption of DPH onto the catalyst. Different DPH concentrations (0, 12.5, 25, 50, 75 and 100 mg/L) were prepared with 0.4 g TiO<sub>2</sub>/L, at the natural pH (pH ≈ 6.0 ± 0.2) and constant temperature (25 °C ± 0.5). After 1, 5 and 24 h of contact, DPH concentration was evaluated. Adsorption does not play an important role in the photocatalytic processes in this case, as shown in Fig. 1.

**Table 1**

Technical characteristics of the pilot plant (CPCs).

REACTOR: CPC	
Collector geometry	Compound Parabolic Collector (CPC)
Collector material	Al-reflective mirrors
Mirrors area (m <sup>2</sup> )	0.228
Light source	Solar light
Photoreactors number (number of tubes)	6
Photon flux	Depending of day (290–400 nm)
Glass material	Quartz
Length of each photoreactor (cm)	56
Inner diameter of photoreactors (cm)	1.75
Wall thickness of photoreactors (cm)	0.15
Total volume of photoreactor (L)	0.95
Total volume of suspension (L)	10
Volume irradiated (L)	0.95
Volume irradiated/Volume dark (%)	9.5
Temperature (°C)	30 ± 5
Stirring system	Mechanic external
Volumetric flow rate (L/min)	2.6
Place localization (coordinates)	At sea level Barcelona
Inclination (°)	(Latitude 41°28', Longitude 2°06')

On the other hand, photolysis experiments were carried out with 50 mg/L of initial DPH in the different reactors (25 ± 5 °C). The results (Table 2) confirmed the low influence of photolysis on DPH degradation in Solarbox, CPC and BLB (2.45%, 1.38% and 4.66%, respectively). Only UVC light is powerful enough to break the DPH bonds because UVC light covers the range of light adsorption of DPH ( $\lambda_{\max}$  at 220 nm). UVC light is able to degrade 36.5% of initial DPH in 60 min with a quantum yield ( $\Phi$ ) of 0.033 mol/Einstein. Moreover, photolysis did not promote relevant mineralization.

### 3.2. Light/H<sub>2</sub>O<sub>2</sub> experiments under different radiation sources

All experiments have been carried out with 50 mg/L of DPH and different concentrations of H<sub>2</sub>O<sub>2</sub> (15, 75 or 150 mg/L) under different radiation sources (UV-C, BLB and simulated solar radiation). The optimal concentration of peroxide for all the experimental devices was 150 mg/L, because the highest amount of peroxide generates the highest amount of OH· radicals. As it can be observed in Table 3, in all the experiments, a very low mineralization was reached. The highest TOC conversion was 10.7% with 150 mg/L of H<sub>2</sub>O<sub>2</sub> under UV-C, 14.5 kJ/L of radiation, after 60 min of irradiation.

As it can be observed in Fig. 2 and 100% DPH degradation was achieved at 20 min under UV-C with the highest concentration of hydrogen peroxide studied. This can be related to the direct photolysis of DPH, 37% of total DPH can be removed under UV-C, and the hydrogen peroxide photolysis, because UV-C radiation is powerful enough to break H<sub>2</sub>O<sub>2</sub> quickly and produce two hydroxyl radicals.

### 3.3. Fenton and photo-Fenton process

In Fenton and photo-Fenton processes, two different pHs have been studied in order to compare the efficiency of the processes: acid pH (2.8) and initial circumneutral pH (6.2).

At acid pH experiments, the reactor was fed with DPH solution (50 mg/L) and pH was adjusted to 2.8 with H<sub>2</sub>SO<sub>4</sub> to avoid iron precipitation. In contrast, for the experiments at initial circumneutral pH, the acidification of DPH solution (50 mg/L) is avoided by the addition of resorcinol (50 mg/L of RES), which is used to simulate organic matter.

Table 4 summarizes the results obtained for dark-Fenton process carried out in dark and room temperature conditions at two pHs (2.8 and 6.2). Two concentrations of Fe<sup>2+</sup> (2.5 and 5 mg/L) and H<sub>2</sub>O<sub>2</sub> (15 and 150 mg/L) were tested. It can be observed the positive influence of iron and H<sub>2</sub>O<sub>2</sub> in DPH abatement. 100% DPH conversion was achieved with 150 mg/L H<sub>2</sub>O<sub>2</sub> and 5 mg/L Fe<sup>2+</sup>, at acid pH and initial circumneutral pH. The presence of resorcinol,

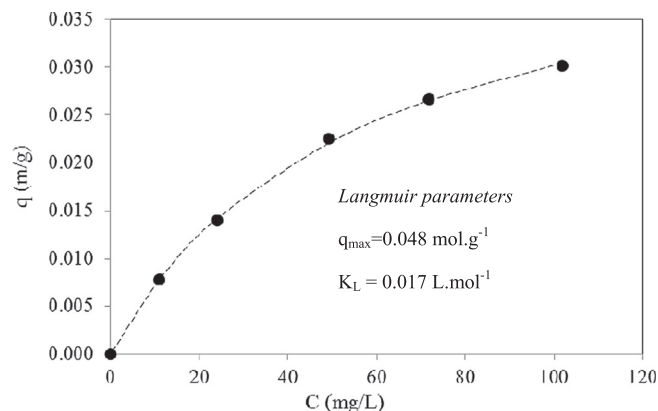


**Fig. 1.** Adsorption of DPH on TiO<sub>2</sub> particles (● experimental values and – Langmuir-Hishelwood isotherm model).

**Table 2**  
DPH and TOC removal at 60 min in the different photo-reactors.

Radiation source	DPH (%) removed at 60 min	TOC (%) removed at 60 min	Q (kJ/L) (290–400 nm) at 60 min
UVC	36.5	3.37	14.4
BLB	4.66	4.50	3.59
SB	2.45	1.96	12.9
CPC	1.38	0.90	7.86

**Table 3**  
DPH and TOC removal at 60 min in different photo-reactors by light/H<sub>2</sub>O<sub>2</sub> process.

Radiation source	H <sub>2</sub> O <sub>2</sub> (mg/L)	DPH (%) removed at 60 min	TOC (%) removed at 60 min	Q (kJ/L) (290–400 nm) at 60 min
UVC	15	85.5	1.92	14.4
	75	98.7	4.20	14.4
	150	100	10.7	14.4
BLB	15	5.00	2.25	3.59
	75	7.37	2.45	3.59
	150	15.2	2.84	3.59
SB	15	4.47	0.68	12.9
	75	5.39	1.72	12.9
	150	6.00	2.31	12.9
CPC	15	2.16	1.34	7.78
	75	7.37	1.05	7.87
	150	10.9	3.61	8.03

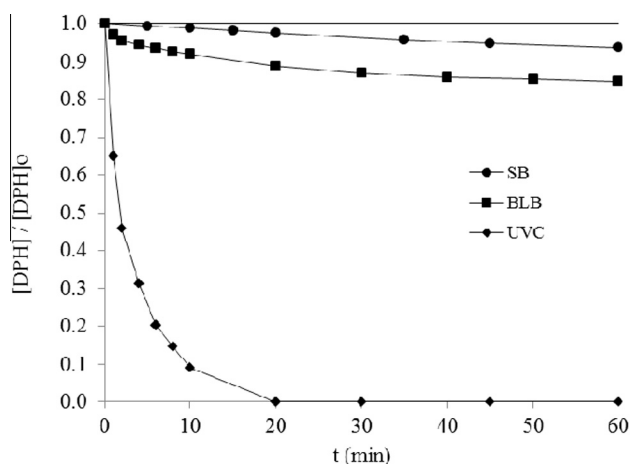


**Fig. 2.** DPH degradation by light/H<sub>2</sub>O<sub>2</sub> process. [DPH]<sub>0</sub> = 50 mg/L, [H<sub>2</sub>O<sub>2</sub>] = 150 mg/L.

**Table 4**  
DPH and TOC removal at 60 min for acid pH and initial circumneutral pH in Fenton process.

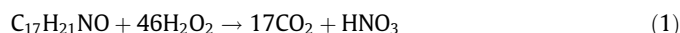
pH	H <sub>2</sub> O <sub>2</sub> (mg/L)	Fe <sup>2+</sup> (mg/L)	DPH (%) at 60 min	TOC (%) at 60 min
2.8	15	2.5	60.4	6.54
	15	5	60.9	9.82
	150	2.5	56.1	18.1
	150	5	96.7	19.5
6.2	15	2.5	60.7	14.1
	15	5	76.7	15.7
	150	2.5	100	22.8
	150	5	100	31.0

with a chelating effect, avoids the precipitation of Fe<sup>3+</sup> hydroxy complexes at neutral pH, providing a positive effect on Fenton. The mineralization reached was 31.0%. This TOC conversion is low but higher than the mineralization at acid pH (19.5%). It could

be due to the formation of Fe-RES complexes that can accelerate the reduction of Fe<sup>3+</sup> to Fe<sup>2+</sup> as well as the formation of OH<sup>•</sup> from H<sub>2</sub>O<sub>2</sub> decomposition [17,18].

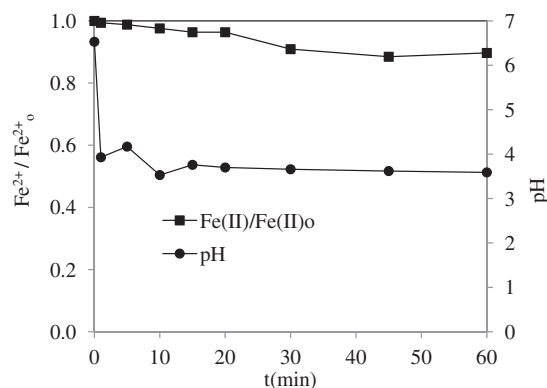
As it can be observed in Fig. 3, at the beginning of the treatment, the pH drops from 6.2–3.6 and it keeps constant during the irradiation time, as result of the acidic nature of the RES by-products in the media. The decrease in pH slows the rate of iron (II) oxidation by O<sub>2</sub> [19], and it may be the reason for the presence of the ferrous iron in solution during all the reaction time. In addition, we can assume that the by-products form complexes with iron (III) allowing its solubilisation [6,10,11,20]. The initial pH (6.2) of the solution subserve RES degradation, suggesting that it could be mainly catalysed by iron-carboxylic acid complexes [9,19]. The Fenton process has the drawback that the regeneration of ferrous iron from ferric iron is the rate limiting step in the catalytic iron cycle. However, using the resorcinol, there was ferrous iron in the media during the treatment.

Photo-Fenton experiments were carried out using different photo-reactors with different Fe<sup>2+</sup> (2.5 or 5 mg/L) and H<sub>2</sub>O<sub>2</sub> (15 or 150 mg/L) concentrations. As it can be observed in Table 5, within 20 min with the highest iron and hydrogen peroxide concentrations, a complete DPH degradation was obtained at acid pH (5 min for UV-C, 10 min for BLB and 20 min for SB). Moreover, in these conditions, the highest values of mineralization have been found (35.9%, 32.5% and 23.6% for UV-C, BLB and SB, respectively). The use of stoichiometric H<sub>2</sub>O<sub>2</sub> concentration does not allow the total DPH conversion but an excess of hydrogen peroxide (mg H<sub>2</sub>O<sub>2</sub>/mg MET ratio = 3) allows the total conversion of DPH. It means that the optimal H<sub>2</sub>O<sub>2</sub> concentration is higher than the stoichiometric dosage (46 mol of H<sub>2</sub>O<sub>2</sub>). Although total DPH conversion is achieved, it doesn't ensure a total mineralization [21]:



In general, TOC reduction slightly increases (from 6.74% to 9.81% for photo-Fenton at acid pH with 15 mg/L of H<sub>2</sub>O<sub>2</sub>) with catalyst load (from 2.5 mg/L to 5 mg/L of Fe<sup>2+</sup>, respectively). The iron concentration never has been higher than the limit indicated by European Union standards for discharge of treated waters (i.e. 5 mg/L in Spain).

As it can be observed in the Fig. 4, the highest conversion of DPH was obtained at the highest iron and hydrogen peroxide concentrations in UV-C and BLB photo-reactor. A reason to justify those differences refers to the spectrum of the light used at each installation. Spectrum of light used in SB reactor corresponds to the solar one, wider and richer in longer wavelengths. Considering the spectrum range below 500 nm, the most of photons (~80%) are in the 400–500 nm stretch and only 20% of photons are below 400 nm. Although light over 400 nm can be useful for photo-



**Fig. 3.** Trend of Fe<sup>2+</sup> and pH in the experiments carried out with 50 mg/L of DPH and 50 mg/L of RES during the Fenton process at initial circumneutral pH (6.2).



**Table 5**  
DPH and TOC removal at 60 min in in photo-Fenton process at acid pH (2.8).

Radiation source	H <sub>2</sub> O <sub>2</sub> (mg/L)	Fe <sup>2+</sup> (mg/L)	DPH (%) removed at 60 min	TOC (%) removed at 60 min	Q (kJ/L) (290–400 nm) at 60 min	HPD removed/Energy (mg/kJ)
UVC	15	2.5	97.5	13.4	14.5	6.72
	15	5	100	13.8	14.5	6.90
	150	2.5	100	30.5	14.5	6.90
	150	5	100	35.9	14.5	6.90
BLB	15	2.5	96.5	10.5	3.59	26.9
	15	5	97.8	12.6	3.59	27.2
	150	2.5	100	28.7	3.59	27.9
	150	5	100	32.5	3.59	27.9
SB	15	2.5	90.4	6.74	12.9	7.01
	15	5	94.8	9.81	12.9	7.35
	150	2.5	100	20.7	12.9	7.75
	150	5	100	23.6	12.9	7.75

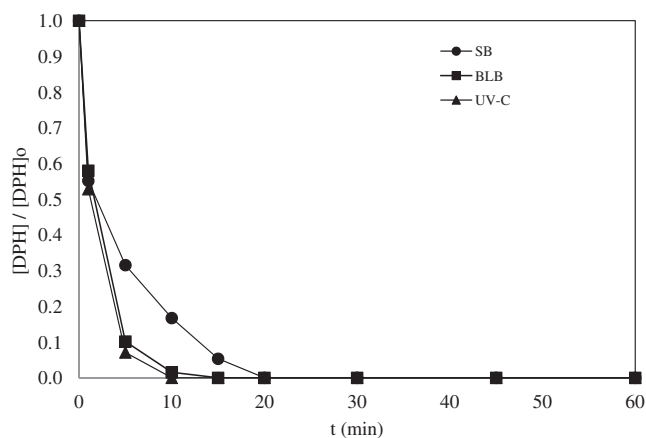


**Fig. 4.** DPH degradation by photo-Fenton process. [DPH]<sub>0</sub> = 50 mg/L, [H<sub>2</sub>O<sub>2</sub>] = 150 mg/L, [Fe<sup>2+</sup>] = 5 mg/L, acid pH.

Fenton process, it is much less efficient. It means that a huge part of the considered radiation may not being used, decreasing the overall yield of the process. On the other hand, UVC and BLB reactors operate in a radiation range much more efficient for photo-Fenton and the process takes place in vessels with the lamps located in the axis of them, ensuring the full absorption of the irradiated light [22]. Furthermore, in UV-C system the influence of the photolysis may be important (37% of total DPH can be removed). In addition, as commented before, UV-C radiation is powerful enough to break H<sub>2</sub>O<sub>2</sub> quickly and produce two hydroxyl radicals.

The efficiency of photo-Fenton process at circumneutral pH was also compared with the classical photo-Fenton process at acid pH with BLB lamps. As it can be observed in Fig. 5 and 100% of DPH degradation was achieved with 5 mg Fe<sup>2+</sup>/L and 150 mg H<sub>2</sub>O<sub>2</sub>/L at 15 min for acid pH and 20 min for circumneutral pH. Using 2.5 mg Fe<sup>2+</sup>/L and 150 mg H<sub>2</sub>O<sub>2</sub>/L, 100% of DPH degradation at acid pH and 99.3% of DPH conversion at circumneutral pH was observed at 60 min. Moreover, 97.8 and 94.1% of DPH conversion was obtained with 5 mg Fe<sup>2+</sup>/L and 15 mg H<sub>2</sub>O<sub>2</sub>/L at acid pH and neutral pH, respectively during the first 60 min of reaction. Finally, 96.5% and 90.5% with 2.5 mg Fe/L and 15 mg H<sub>2</sub>O<sub>2</sub>/L at acid pH and initial circumneutral pH, respectively, was observed at 60 min. The complete DPH degradation was reached using the highest concentrations of Fe<sup>2+</sup> and H<sub>2</sub>O<sub>2</sub>.

Regarding TOC conversion (Table 6), photo-Fenton process at initial circumneutral pH achieved conversions around 38.6% at highest concentrations of Fe<sup>2+</sup> (5 mg/L) and H<sub>2</sub>O<sub>2</sub> (150 mg/L), whereas the conversion achieved at acid pH was around 32%. Thus, a slightly improvement can be observed at initial neutral pH.

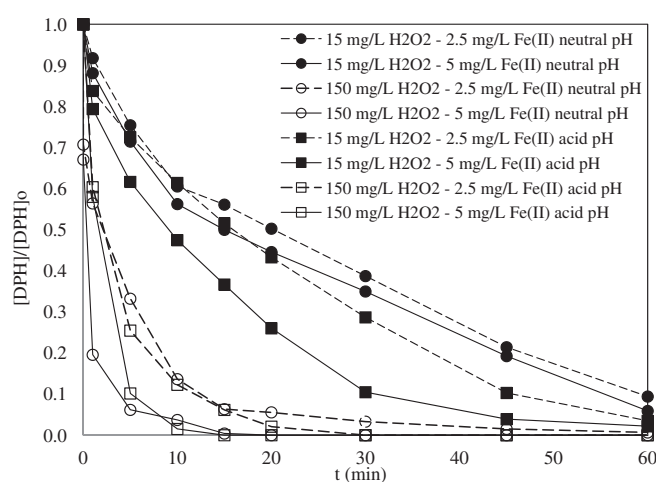


**Fig. 5.** DPH degradation by photo-Fenton process at acid pH and initial circumneutral pH under BLB lamps.

Fenton and photo-Fenton were compared at pH 2.8 and at initial circumneutral pH for 5 mg/L of Fe<sup>2+</sup> and 150 mg/L H<sub>2</sub>O<sub>2</sub> (Fig. 6). A complete DPH depletion was obtained by Fenton at circumneutral pH in 30 min and 67% of DPH conversion was achieved with Fenton at pH 2.8. RES can interact with the iron ion and hence can greatly influence the mechanism and kinetics of the Fenton reaction by the formation of hydroxyl radicals. In this way, Fe<sup>3+</sup> is reduced by resorcinol to Fe<sup>2+</sup> and resorcinol is oxidized to semiquinone radical anion. Oxygen is reduced to superoxide (O<sub>2</sub><sup>-</sup>) and semiquinone forms quinone. Superoxide is then transformed to hydrogen peroxide which reacts with Fe<sup>2+</sup> by Fenton reaction to produce more reactive hydroxyl radicals [23].

In photo-Fenton, with resorcinol, a complete DPH elimination was obtained in 20 min of irradiation and 15 min of irradiation

**Table 6**  
TOC removal in photo-Fenton process at circumneutral pH.

pH	H <sub>2</sub> O <sub>2</sub> (mg/L)	Fe <sup>2+</sup> (mg/L)	% TOC removed at 60 min
2.8	15	2.5	10.1
	15	5	12.6
	150	2.5	28.7
	150	5	32.5
6.2	15	2.5	16.4
	15	5	18.1
	150	2.5	30.8
	150	5	38.6

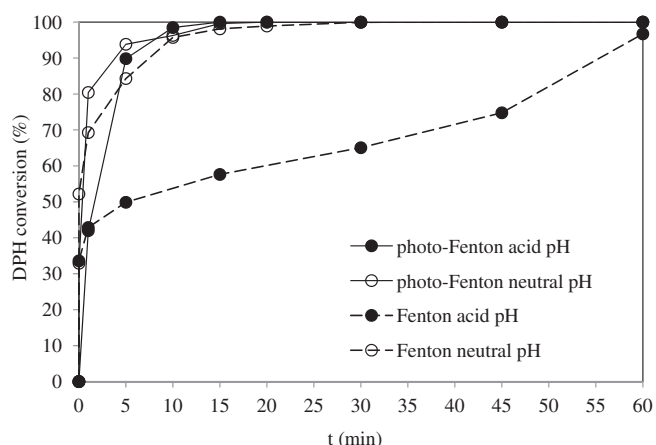


Fig. 6. DPH degradation by Fenton (---) and photo Fenton (—) process at acid pH (●) and circumneutral pH (○).

were necessary without resorcinol and pH 2.8. The Fig. 6 shows the enhancement of the photo-Fenton process at initial time when the experiments were carried out with resorcinol in the media. The presence of resorcinol has a chelating effect, thus, the positive effect of natural organic matter (NOM) on Fenton systems has been confirmed. Moreover, the use of NOM in the reaction medium allows to work at near neutral pH obtaining almost the same efficiency as working at acid pH [6,9,11,24,25]. Another aspect is that, during the reaction, OH<sup>•</sup> attacked both DPH and RES, but there is not complexes destruction because no loss of iron was observed [26].

### 3.4. Photocatalysis experiments

Three different catalyst loads were assessed (0.05, 0.1 and 0.4 g/L TiO<sub>2</sub>) in SolarBox to choose the optimum catalyst concentration for further comparison with other photo-reactors. As it can be observed in Table 7, the best results, for DPH degradation, were obtained with 0.4 g TiO<sub>2</sub>/L. Higher TiO<sub>2</sub> concentrations were also tested but TiO<sub>2</sub> settling in the reactor was observed. Therefore, those higher catalyst amounts were discarded, because TiO<sub>2</sub> settling in the reactor could increase radiation scattering, decreasing the reaction rate. The optimal loading depends on the photoreactor geometry and operation conditions [27]. Some researchers found that P25 TiO<sub>2</sub> catalyst is very efficient at low catalyst loadings (i.e. 0.03, 0.05, 0.25 and 0.5 g/L) [27]. DPH mineralization varying catalyst concentration was also investigated. Mineralization achieved was really low: 4.5, 6.6 and 9.8% of TOC conversion was obtained for 0.05, 0.1 and 0.4 g TiO<sub>2</sub>/L, respectively, after 60 min

of irradiation in SB reactor. The effect of H<sub>2</sub>O<sub>2</sub> addition, as promoter, was evaluated with 0.4 g/L of catalyst in SB and CPC devices. For this purpose, 15 or 150 mg/L of H<sub>2</sub>O<sub>2</sub> were added to 50 mg/L DPH solution directly in the batch tank. The highest degradation of DPH was obtained with 150 mg/L of H<sub>2</sub>O<sub>2</sub>: 62.6% and 53.9% of DPH conversion in SB and CPC, respectively. The joint presence of UV, H<sub>2</sub>O<sub>2</sub> and TiO<sub>2</sub> (UV-vis/H<sub>2</sub>O<sub>2</sub>/TiO<sub>2</sub> process) improves DPH degradation, because peroxide acts as additional source of hydroxyl radicals, improving the overall efficiency. Mineralization levels in this system were low with only 16.2% and 6.71% of TOC conversion, for SB and CPC reactors.

Furthermore, DPH conversion was compared for the four different installations already presented (SB, BLB, UVC, CPC). Experimental conditions used were the same for all the installations: 0.4 g/L of TiO<sub>2</sub> and 50 mg DPH/L at 25 °C. Apart from the geometry, the only difference between the experiments was the type and amount of light irradiating the system. From Table 7, it can be observed that, at the same irradiation time and titania concentration, in the experiments carried out with UV-C and UV-A, the degradation achieved was very close to that obtained in the SB. This can be related to the fact that, in SB and UV-A, TiO<sub>2</sub> absorbs radiation from 380 nm to 400 nm. Although in UV-C there is not absorption of TiO<sub>2</sub> in the 280–300 nm range, the DPH degradation value can be due to its photolysis. The TOC results were not promising and almost equal mineralization was achieved for UV-C, UV-A and SB, 8.71%, 7.42% and 9.80%, respectively. To take into account the radiation effect, degradation is presented as the energy required in the radiation range of titania absorption for the abatement of 1 mg of DPH, after 60 min of irradiation for 0.4 g/L of titania. The required energy to remove 1 mg of DPH is highest for UV-C radiation (0.46 kJ/mg) than the others (0.36, 0.11 and 0.26 kJ/mg for SB, UV-A and CPC, respectively).

### 3.5. Set-ups comparison

In this section the different devices an AOPs tested will be compared at the same time to observe the effect of geometry and light. As commented before, DPH and TOC removal were evaluated in three different experimental devices at laboratory scale: a Solarbox (SB) with a Xe lamp, a reactor (BLB) with three black light lamps and a reactor (UVC) with three UV-C lamps. Experimental conditions were the same in all installations (concentrations of DPH, photocatalyst, iron(II) and hydrogen peroxide). The best results obtained for DPH removal in each experimental device were considered for the comparison of the different installations tested. Giving these premises, the observed differences are only related to the geometry of the reactors and type and amount of light irradiating the systems. The entering radiation was 0.97 J/s in the case of SB, 2.12 J/s for BLB device, and 5.99 J/s for the UV-C reactor (between

Table 7  
Summary of DPH and TOC removal at several experimental conditions.

Radiation source	Ti O <sub>2</sub> (g/L)	H <sub>2</sub> O <sub>2</sub> (mg/L)	DPH (%) removed at 60 min	TOC (%) removed at 60 min	Q (kJ/L) (290–400 nm) at 60 min	Energy/HPD removed (kJ/mg)
SolarBox	0.05	0	15.8	4.52	12.9	0.82
	0.1	0	27.0	6.62	12.9	0.48
	0.4	0	35.7	9.80	12.9	0.36
	0.4	15	48.4	10.9	3.17	0.13
	0.4	150	62.6	16.2	3.17	0.10
BLB	0.4	0	32.5	7.42	3.59	0.11
UVC	0.4	0	31.7	8.71	14.4	0.46
CPC	0.4	0	8.77	5.58	2.28	0.26
	0.4	150	53.9	6.71	7.25	0.33

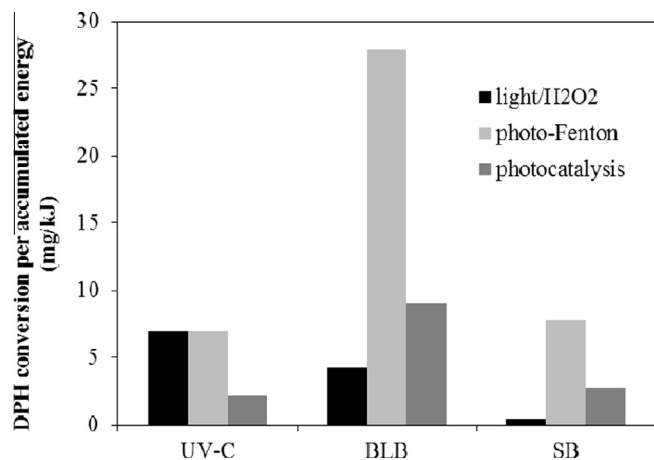


Fig. 7. DPH removal per accumulated energy in UV-C, BLB and SB devices at 60 min.

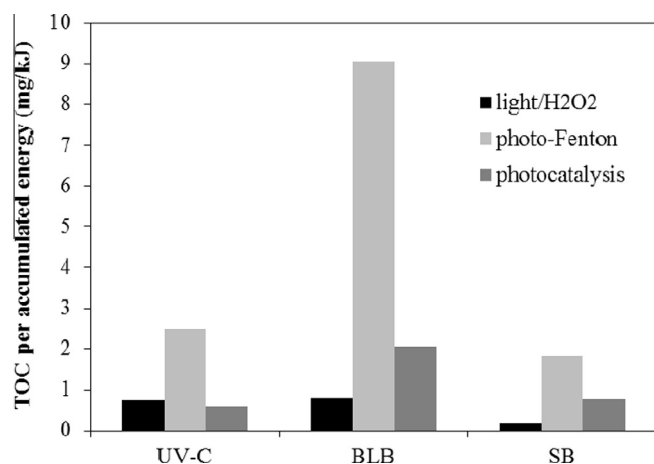


Fig. 8. TOC reduction per accumulated energy in UV-C, BLB and SB devices at 60 min.

290 and 400 nm). The performance of the three set-ups in DPH elimination is compared on basis of the ratio removed DPH/accumulated energy. For better comparison, the DPH conversion at 60 min of reaction was chosen.

As it can be observed in the Fig. 7, photo-Fenton process at acid pH shows an efficiency ratio higher than the other two technologies in DPH conversion. In the UV-C reactor, the degradation rates and accumulated energies used were similar for UV/H<sub>2</sub>O<sub>2</sub> (150 mg/L of H<sub>2</sub>O<sub>2</sub>) and photo-Fenton experiments (5 mg/L of Fe<sup>2+</sup> and 150 mg/L of H<sub>2</sub>O<sub>2</sub>), at 60 min of irradiation. As the UV-C lamps used in this study are monochromatic and emit radiation with a maximum at 254 nm, it is possible that the photolysis of H<sub>2</sub>O<sub>2</sub> has a great influence during the treatment in this device. In addition, the high DPH absorbance at 220 nm seems to be responsible for the good performance of photolysis process in DPH conversion. Photocatalytic process is less effective under UVC radiation, because TiO<sub>2</sub> does not absorb light in the 280–300 nm range.

According to Fig. 7 the BLB reactor exhibits a much better performance than SB reactor and UV-C reactor. A main reason to justify those differences refers to the spectrum of used light at each installation. It was expected that SB would provide a better degradation rate according to the high power of the lamp. However, only radiation below 500 nm is useful in photo-Fenton process, decreasing the total yield of the process (7.75 mg DPH removed/kJ). On the

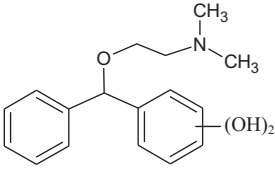
Table 8

DPH and its main intermediates detected by LC/MS analysis in photodegradation experiments.

<i>m/z</i> (Da)	Elemental composition	Proposed structure (Label)
72	C <sub>4</sub> H <sub>10</sub> N	 DPH-72
88	C <sub>4</sub> H <sub>10</sub> NO	 DPH-88
90	C <sub>4</sub> H <sub>12</sub> NO	 DPH-90
120	C <sub>5</sub> H <sub>14</sub> NO <sub>2</sub>	 DPH-120
167	C <sub>13</sub> H <sub>11</sub>	 DPH-167
183	C <sub>13</sub> H <sub>12</sub> O	 DPH-183
194	C <sub>11</sub> H <sub>16</sub> NO <sub>2</sub>	 DPH-194
199	C <sub>13</sub> H <sub>12</sub> O <sub>2</sub>	 DPH-199
256	C <sub>17</sub> H <sub>22</sub> NO	 DPH-256
272	C <sub>17</sub> H <sub>22</sub> NO <sub>2</sub>	 DPH-272

(continued on next page)

Table 8 (continued)

<i>m/z</i> (Da)	Elemental composition	Proposed structure (Label)
288	C <sub>17</sub> H <sub>22</sub> NO <sub>3</sub>	 DPH-288

other hand, UVC and BLB operate in a radiation range much more efficient and the photo-Fenton process works better with the wavelength of the BLB reactor (365 nm) than the UVC reactor (254 nm).

The ratio TOC removal (mg) per accumulated energy (kJ) (see Fig. 8) was also analyzed taking into account the TOC removed in BLB, UVC and SB reactors. The ratio (mg TOC/kJ) obtained in BLB was almost four times higher than in UVC and SB reactors: 9.05, 2.49 and 1.83, respectively.

Therefore, considering the results of both ratios (mg DPH/kJ and mg TOC/kJ), it can be concluded that BLB lamps are more useful for the process than the other used lamps. Photo-Fenton process with 5 mg/L of Fe<sup>2+</sup> and 150 mg/L of H<sub>2</sub>O<sub>2</sub> shows the best results for both degradation and mineralization of DPH by accumulated energy unit.

### 3.6. Intermediates and reaction pathways

During the DPH photodegradation processes, several by-products are produced. To complete the information on these processes, the main intermediates formed in these reactions have been identified by electrospray mass technique (see Table 8).

Hydroxyl radical is reported as a non-selective oxidizing species that mainly undergo by addition reaction on aromatic ring and on alkylamine side chain [28]. In the case of DPH, it is logical to expect the addition of OH<sup>•</sup> to the aromatic ring and the alkylamine side chain, leading to the formation of DPH-272. The hydroxyl addition on alkylamine chain, followed by the benzylic dissociation, leads to the formation of *m/z* 183 (DPH-183) and *m/z* 90 (DPH-90) fragments. However, the hydroxyl addition on alkylamine chain can lead to *m/z* 167 (DPH-176) and *m/z* 89 (DPH-89) fragments by via proton transfer within an intermediate ion-neutral complex [29]. Moreover, the hydroxycyclohexadienyl form of DPH-272 could be attacked by OH<sup>•</sup> in the reaction medium forming a product with a double hydroxyl (DPH-288) [28]. In addition, the DPH-272 form could suffer the dissociation of oxygen from the carbon bond of the ether group leading to *m/z* 199 (DPH-199), by further hydrogenation, or to *m/z* 72 (DPH-72), by an H-abstraction.

The mechanism leading to the formation of DPH-194 compound is initiated by the attack of OH<sup>•</sup> on the ortho position of DPH-256 followed by the elimination of a phenol and subsequent oxidation. Analogous mechanism could explain the formation of DPH-120 compound from DPH-194 [29].

## 4. Conclusions

Concerning the performance of the different processes studied (UV-vis/H<sub>2</sub>O<sub>2</sub>, Fenton, photo-Fenton and heterogeneous photocatalysis with TiO<sub>2</sub>) under different radiation, it is found that photo-Fenton shows the best results in terms of DPH and TOC conversion using the highest Fe<sup>2+</sup> (5 mg/L) and H<sub>2</sub>O<sub>2</sub> (150 mg/L) concentrations with all the radiation sources. The comparisons

between the devices in photo-Fenton process established that BLB reactors show the highest efficiency in the ratio removed DPH/accumulated energy in the range radiation 290–400 nm. The treatment in SB and UV-C reactor seem to be more expensive than the other technologies, because these devices are equipped with a very powerful lamps but only a very small fraction of that energy produce useful radiation for the photo-Fenton process.

The addition of resorcinol allowed working at circumneutral pH. In Fenton process a complete DPH conversion was achieved with 5 mg/L of Fe<sup>2+</sup> and 150 mg/L of H<sub>2</sub>O<sub>2</sub> in presence of resorcinol, whereas, at the same conditions, but at acid pH, 96.7% of DPH conversion was obtained. In photo-Fenton, with resorcinol and without resorcinol, a complete DPH elimination was obtained in 15 min of irradiation and 20 min of irradiation, respectively. In conclusion, the presence of resorcinol has a natural organic matter (NOM) on photo-Fenton systems, exhibits more or less the same degradation as at acid pH, which allows working at near neutral pH and avoiding the consumption of reagents for acidification.

The transformation reaction of DPH establishes that hydroxyl radicals mostly attack the aromatic ring and alkylamine side chain yielding hydroxycyclohexadienyl and alkyaminodiol intermediates. Moreover an ortho attack in the case of OH<sup>•</sup> reaction could be other mechanism of degradation but it is a minor pathway.

## Acknowledgment

The authors thank the Ministry of Science and Innovation of Spain (project CTQ2014-52607-R) and AGAUR-Generalitat de Catalunya (project 2014SGR245) for funding this research. Arsalan Afkhami is grateful to the European Commission for the scholarship funded within the Erasmus+ KA1 Programme, ref. 20130241 Erasmus Mundus Joint Master Degree in Chemical Innovation and Regulation.

## References

- [1] M. Fuerhacker, EU water framework directive and Stockholm convention: can we reach the targets for priority substances and persistent organic pollutants, *Environ. Sci. Pollut. Res. Int.* 16 (Suppl 1) (2009) S92–S97.
- [2] S. Alonso, M. Catalá, R. Maroto, Pollution by psychoactive pharmaceuticals in the Rivers of Madrid metropolitan area (Spain), *Environ. Int.* 36 (2010) 195–201.
- [3] N. Miranda, S. Suárez, I.M. Maldonado, S. Malato, B. Sánchez, Regeneration approaches for TiO<sub>2</sub> immobilized photocatalyst used in the elimination of emerging contaminants in water, *Catal. Today* 230 (2014) 27–34.
- [4] M.J. Gómez, M.J. Martínez-Bueno, S. Lacorte, A.R. Fernández-Alba, A. Agüera, Pilot survey monitoring pharmaceuticals and related compounds in a sewage treatment plant located on the Mediterranean coast, *Chemosphere* 66 (2007) 993–1002.
- [5] M.J. Martínez-Bueno, A. Agüera, M.J. Gómez, M.D. Hernando, J.F. García-Reyes, A.R. Fernández-Alba, Application of liquid chromatography/quadrupole-linear ion trap mass spectrometry and time-of-flight mass spectrometry to the determination of pharmaceuticals and related contaminants in wastewater, *Anal. Chem.* 79 (2007) 9372–9384.
- [6] A. Moraes, A. Schwarz, H. Spinosa, Maternal exposure to diphenhydramine during the fetal period in rats: effects on physical and neurobehavioral development and on neurochemical parameters, *Neurotoxicol. Teratol.* 26 (2004) 681–692.
- [7] V. Roos, L. Gunnarsson, J. Fick, Prioritising pharmaceuticals for environmental risk assessment: towards adequate and feasible first-tier selection, *Sci. Total Environ.* 421–422 (2012) 102–110.
- [8] I. Sirés, E. Brillas, Remediation of water pollution caused by pharmaceutical residues based on electrochemical separation and degradation technologies: a review, *Environ. Int.* 40 (2012) 212–229.
- [9] E. Ortega-Gómez, B.E. García, M.M. Ballesteros, P. Fernández, J.A. Sánchez, Inactivation of *Enterococcus faecalis* in simulated wastewater treatment plant effluent by solar photo-Fenton at initial neutral pH, *Catal. Today* 209 (2013) 195–200.
- [10] E. Ortega-Gómez, M.M. Ballesteros, B.E. García, J.A. Sánchez, P. Fernández, Solar photo-Fenton for water disinfection: an investigation of the competitive role of model organic matter for oxidative species, *Appl. Catal. B* 148 (2014) 484–489.
- [11] D. Spuhler, J.A. Rengifo-Herrera, C. Pulgarin, The effect of Fe<sup>2+</sup>, Fe<sup>3+</sup>, H<sub>2</sub>O<sub>2</sub> and the photo-Fenton reagent at near neutral pH on the solar disinfection (SODIS)



- at low temperatures of water containing *Escherichia coli* K12, *Appl. Catal. B* 96 (2010) 126–141.
- [12] D.G. Larsson, C. de Pedro, N. Paxeus, Effluent from drug manufactures contains extremely high levels of pharmaceuticals, *J. Hazard. Mater.* 148 (2007) 751–755.
- [13] E.K. Putra, R. Pranowo, J. Sunarso, W. Indraswati, S. Ismadji, Performance of activated carbon and bentonite for adsorption of amoxicillin from wastewater: mechanism, isotherms and kinetics, *Water Res.* 43 (2009) 2419–2430.
- [14] R.F. Pupo Nogueira, M.C. Oliveira, W.C. Paterlini, Simple and fast spectrophotometric determination of  $H_2O_2$  in photo-Fenton reactions using metavanadate, *Talanta* 66 (2005) 86–89.
- [15] H.J. Kuhn, S.E. Braslavsky, R. Schmidt, Chemical actinometry (IUPAC Technical Report), *Pure. Appl. Chem.* 76 (2004) 2105–2146.
- [16] N. De la Cruz, V. Romero, R.F. Dantas, P. Marco, B. Bayarri, J. Giménez, S. Esplugas, O-Nitrobenzaldehyde actinometry in the presence of suspended  $TiO_2$  for photocatalytic reactors, *Cat. Today* 209 (2013) 209–214.
- [17] L. Chen, J. Ma, X. Li, J. Zhang, J. Fang, Y. Guan, P. Xie, Strong enhancement on fenton oxidation by addition of hydroxylamine to accelerate the Ferric and Ferrous, *Iron Cycl. Environ. Sci. Technol.* 45 (2011) 3925–3930.
- [18] Z. Ma, L. Ren, S. Xing, Y. Wu, Y. Gao, Sodium dodecyl sulfate modified  $FeCo_2O_4$  with enhanced Fenton-like activity at neutral pH, *J. Phys. Chem. C* 119 (2015) 23068–23074.
- [19] J.F. Barona, D.F. Morales, L.F. González-Bahamón, C. Pulgarín, L.N. Benítez, Shift from heterogeneous to homogeneous catalysis during resorcinol degradation using the solar photo-Fenton process initiated at circumneutral pH, *Appl. Catal. B* 165 (2015) 620–627.
- [20] A. Moncayo-Lasso, J. Sanabria, C. Pulgarín, N. Benítez, Simultaneous *E. coli* inactivation and NOM degradation in river water via photo-Fenton process at natural pH in solar CPC reactor. A new way for enhancing solar disinfection of natural water, *Chemosphere* 77 (2009) 296–300.
- [21] L.M. Pastrana-Martínez, N. Pereira, R. Lima, J.L. Faria, H.T. Gomez, A.M.T. Silva, Degradation of diphenhydramine by photo-Fenton using magnetically recoverable iron oxide nanoparticles as catalyst, *Chem. Eng. J.* 261 (2015) 45–52.
- [22] V. Romero, O. Gonzalez, B. Bayarri, P. Marco, J. Giménez, S. Esplugas, Degradation of Metoprolol by photo-Fenton: Comparison of different photoreactors performance, *Chem. Eng. J.* 283 (2016) 639–648.
- [23] J. Prousek, E. Palacková, S. Priesolová, L. Marková, A. Alevov, Fenton- and Fenton-like AOPs for wastewater treatment: From laboratory-to-plant-scale, *Appl. Sep. Sci. Technol.* 42 (2007) 1505–1520.
- [24] A. Georgi, A. Schierz, U. Trommler, C. Horwitz, T. Collins, F. Kopinke, Humic acid modified Fenton reagent for enhancement of the working pH range, *Appl. Catal. B* 72 (2007) 26–36.
- [25] J. Rodríguez-Chueca, M. Polo-López, R. Mosteo, M. Ormad, P. Fernández-Ibáñez, Disinfection of real and simulated urban wastewater effluents using a mild solar photo-Fenton, *Appl. Catal. B* 150 (2014) 619–629.
- [26] A. De Luca, R.F. Dantas, S. Esplugas, Assessment of iron chelates efficiency for photo-Fenton at neutral pH, *Water Res.* 61 (2014) 232–242.
- [27] L.M. Pastrana-Martínez, J.L. Faria, J.M. Doña-Rodríguez, C. Fernández-Rodríguez, A.M.T. Silva, Degradation of diphenhydramine pharmaceutical in aqueous solutions by using two highly active  $TiO_2$  photocatalyst: operating parameters and photocatalytic mechanism, *Appl. Catal. B: Environ.* 113–114 (2012) 221–227.
- [28] S.P.M. Menachery, O. Laprêvote, T.P. Nguyen, U.K. Aravind, P. Gopinathan, C.T. Aravindakumar, Identification of position isomers by energy-resolved mass spectrometry, *J. Mass Spectrom.* 50 (2015) 944–950.
- [29] S.P.M. Menacheru, S.R. Nair, P.G. Nair, U.K. Aravind, C.T. Aravindakumar, Transformation reactions of radicals from the oxidation of diphenhydramine: pulse radiolysis and mass spectrometric studies, *Electro Phys. Theor. Chem.* 5 (2016) 924–933. *Chemistry Select.*